

Robust Tracking and Behavioral Modeling of Movements of Biological Collectives from Ordinary Video Recordings

Hiroki Sayama^{*†}, Farnaz Zamani Esfahlani^{*}, Ali Jazayeri[‡] and J. Scott Turner[§]

^{*}Center for Collective Dynamics of Complex Systems / Department of Systems Science and Industrial Engineering
Binghamton University, State University of New York, Binghamton, NY 13902-6000

[†]Faculty of Commerce, Waseda University, Shinjuku, Tokyo 169-8050, Japan

[‡]Department of Information Science, College of Computing & Informatics, Drexel University, Philadelphia, PA 19104

[§]Department of Biology, SUNY College of Environmental Science and Forestry, Syracuse, NY 13210

Email: sayama@binghamton.edu

Abstract—We propose a novel computational method to extract information about interactions among individuals with different behavioral states in a biological collective from ordinary video recordings. Assuming that individuals are acting as finite state machines, our method first detects discrete behavioral states of those individuals and then constructs a model of their state transitions, taking into account the positions and states of other individuals in the vicinity. We have tested the proposed method through applications to two real-world biological collectives: termites in an experimental setting and human pedestrians in a university campus. For each application, a robust tracking system was developed in-house, utilizing interactive human intervention (for termite tracking) or online agent-based simulation (for pedestrian tracking). In both cases, significant interactions were detected between nearby individuals with different states, demonstrating the effectiveness of the proposed method.

I. INTRODUCTION

Motion tracking and behavioral modeling of biological collectives, such as bird flocks, fish schools, insect swarms, and pedestrian crowds, have been the subject of active research in behavioral ecology [1], [2], [3], [4] and artificial life [5], [6], [7]. This is arguably one of the most challenging tasks in complex systems science, in which researchers need to elucidate unknown microscopic rules that are responsible for the observed or desired macroscopic emergent behaviors.

Previous literature on this topic was mostly focused on modeling individual behaviors in isolation or in response to other individuals in the vicinity through simple kinetic interaction rules. A commonly adopted assumption is that the same set of behavioral rules applies to all individuals homogeneously over space and time, while not much attention was paid to modeling and analyzing multiple distinct behavioral states and their interactions in the collective. However, considering the possibility of multiple behavioral states and their interactions would make the models closer to real biological collectives, where individuals are not acting like non-living particles but can switch from one behavior to another dynamically [8].

The objective of the present study is to (a) propose and evaluate a new, generalizable computational method to detect

and model multiple distinct behavioral states and their interactions among individuals from their externally observable spatio-temporal trajectories, and to (b) develop robust motion tracking systems that can generate trajectory data from ordinary, low-resolution video recordings of real-world biological collectives. In what follows, we first describe the foundational theoretical method of behavioral modeling, and then discuss two versions of robust tracking systems that were developed and tested through applications with two real-world examples of biological collectives: termites and human pedestrians.

II. METHOD FOR BEHAVIORAL MODELING

In this section, we describe theoretical details of the proposed behavioral modeling method. We construct a stochastic model of behavioral transitions of individuals that depend on both the internal state of the individual and the external environmental context, including presence and states of other individuals nearby.

The proposed method analyzes the following observational data for each individual i in population S ($i \in S$; S can vary over time):

- $\vec{x}_i(t)$: Position of individual i at time t
- $E_i(t)$: Local environmental condition for individual i at time t

Here, $E_i(t)$ may include other individuals ($\{\vec{x}_{j \neq i}(t)\}$) and other environmental constraints (e.g., obstacles placed in the space, etc.) that are present in the vicinity of individual i . The spatial/temporal radii that determine the “local environment” are important parameters, which will depend on the specific nature of the collective under investigation. Note that these two pieces of data, $\vec{x}_i(t)$ and $E_i(t)$, are purely observational, described from the viewpoint of an observer/experimenter outside the collective.

Our objective is to computationally convert these observational data into a more dynamical, rule-based description of the collective behavior, with possible interactions among the individuals also adequately captured. To facilitate this challenging task, we adopt a *finite state machine* assumption,

i.e., that the states of individuals in the collective are discrete and finite, and that they can change dynamically according to the input coming from their local environment [8].

The proposed method consists of the following two steps:

A. Step 1. Identifying discrete behavioral states

The objective of this step is to construct the following behavioral state function for each individual i at time t :

$$b_i(t) = \mathcal{L}(\vec{x}_i, E_i)(t) \quad b_i(t) \in B \quad (1)$$

Here, B is a set of discrete behavioral states, and the operator \mathcal{L} applies predefined mathematical operations or computational algorithms to the time series data \vec{x}_i and E_i (not necessarily just their localized values at time t) and produces a behavioral state function b_i . Examples of \mathcal{L} include clustering analyses applied to the frequency components of a short segment of $\vec{x}_i(t)$ around t (used in the first application), and to the velocity vectors of individuals at t (used in the second application). Specific choices of \mathcal{L} will depend on the properties of the collective being analyzed.

We also note that, once $b_i(t)$ has been calculated for i and t , it can be embedded into $E_i(t)$ and second-order (and higher-order) behavioral state functions could be calculated recursively using the updated $E_i(t)$. While this is interesting from a “theory of mind” viewpoint, we did not do such recursive, higher-order behavioral state identification in the present study. However, the first-order behavioral states $b_i(t)$ were embedded in $E_i(t)$ for the following “Building state transition rules” step, in order to detect local interactions of individuals that were specific to their states.

B. Step 2. Building state transition rules

The objective of this step is to construct rules of state transitions that were observed in $b_i(t)$, using $\vec{x}_i(t)$ and $E_i(t)$. Because of the large amount of stochasticity typically present in the observational data, it is reasonable to assume that the transition rules are described in the form of state transition probabilities. This can be written mathematically as follows:

$$\vec{p}_i(t + \Delta t) \approx \mathcal{T}(\vec{x}_i(t), b_i(t), E_i(t)) \quad (2)$$

Here, $\vec{p}_i(t + \Delta t)$ is the probability vector with dimension $|B|$, which represents the probability distribution of the next state of individual i after a short period of time Δt , and \mathcal{T} represents the state transition rules that receive the current position, behavioral state, and local environment of individual i and generate $\vec{p}_i(t + \Delta t)$. Unlike \mathcal{L} in the first step, \mathcal{T} is an unknown mechanism that is to be estimated in this second step, and some heuristic assumptions would be needed to make this estimation task manageable.

In the present study, we assumed that the state transitions would not depend on the position of the individual (this eliminates $\vec{x}_i(t)$ in Eq. (2)), and that \mathcal{T} would simply be a matrix uniquely defined for each behavioral state (which we call $T_{b_i(t)}$ hereafter) that generates $\vec{p}_i(t + \Delta t)$ when multiplied with an environment vector $E_i(t) = \vec{e}_i(t)$. The



Fig. 1. A swarm of 26 individuals of termite species *Macrotermes michaelseni* moving in a Petri dish.

contents of $\vec{e}_i(t)$ will depend on specific applications. With these assumptions, Eq. (2) is simplified as follows:

$$\vec{p}_i(t + \Delta t) \approx T_{b_i(t)} \vec{e}_i(t) \quad (3)$$

This simplification was partly based on our earlier work on morphogenetic swarm chemistry [8]. With this simplification, the estimation of \mathcal{T} becomes a simple least squares estimation of $T_{b_i(t)}$ for each $b_i(t)$, where $\vec{p}_i(t + \Delta t)$ and $\vec{e}_i(t)$ are given in the observational data.

Overall, the final result of this step is given as a $|B| \times |B| \times m$ tensor $\hat{T} = (T_1 T_2 \dots T_{|B|})$, where m is the number of elements in the environment vector $\vec{e}_i(t)$.

III. APPLICATION I: DETECTING INTERACTIONS AMONG TERMITES

We first tested the proposed method through an application to a small-sized population of termites in a well-controlled experimental setting in a laboratory. The objective of this task was to detect interactions among a fixed number (26, specifically) of individuals of termite species *Macrotermes michaelseni* moving in a Petri dish (Fig. 1).

In order to detect and track the positions of individual termites robustly from a low-resolution video recording, we developed an interactive, semi-automated tracking system using Wolfram Research Mathematica’s image feature tracking functions (Fig. 2) [9]. A human user manually enters the initial positions of individuals, and then continuously monitors the automated feature tracking process conducted by Mathematica. When tracking goes wrong, either the human user pauses the system and corrects the positions of tracked individuals, or the system pauses itself and asks the human user for corrections. This hybrid approach integrating automated tracking by a computer and interactive intervention by a human observer

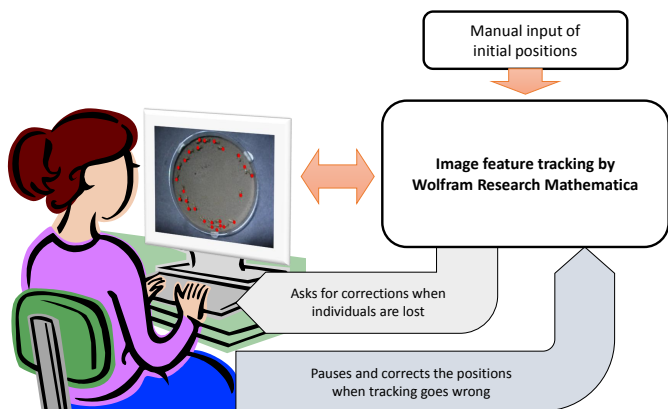


Fig. 2. Interactive, semi-automated tracking system for the first application (tracking termites) developed using Wolfram Research Mathematica's image feature tracking functions.

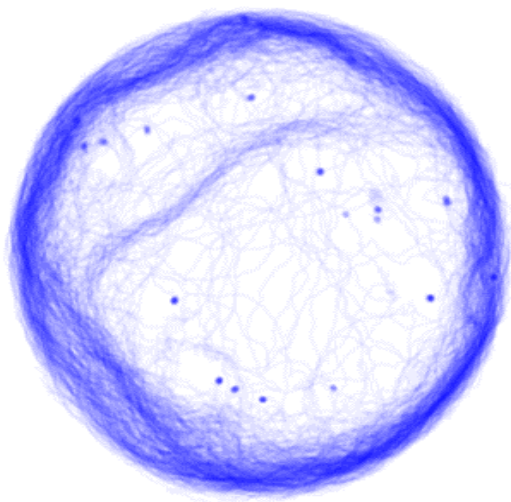


Fig. 3. Trajectories of termites detected using the interactive tracking system, visualized for all the individuals at once. Termite individuals were circling near the edge of the Petri dish most of the time, but some interesting emergent trails were also revealed.

resulted in an effective, low-cost, robust solution that can work with ordinary low-resolution video recordings.

Using the developed tracking system, we converted the video recording into a set of positional time series data, which already showed some interesting emergent trails inside the Petri dish (Fig. 3). It was also observed that the termites' activities characterized by the average speed decreased over time, eventually converging at a low stationary level (Fig. 4).

For identification of discrete behavioral states, we calculated power spectra of short segments (1,000 frames corresponding to about 30 seconds) of the trajectory for each individual around each time point, and extracted the following two metrics from each spectrum: (1) total power of ten lowest frequency components, and (2) peak frequency. Clustering analysis applied to the two-dimensional behavioral feature space created by these two metrics revealed several distinct clusters, which we classified into three behaviors: non-moving,

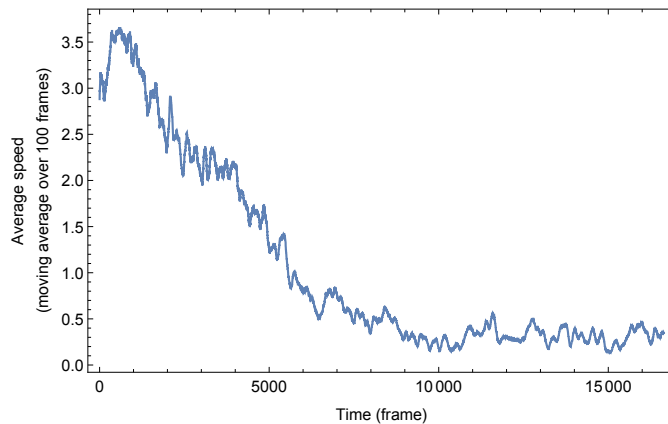


Fig. 4. Temporal change of activities of termites characterized by their average speed. Their activities decreased over time and eventually converged at a low stationary level.

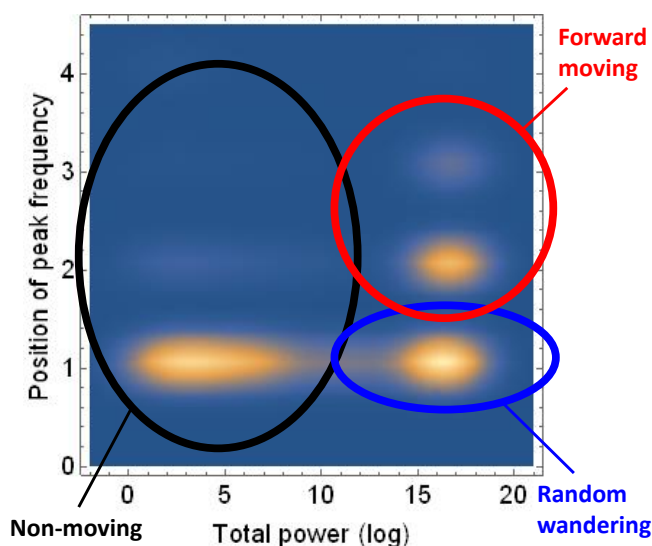


Fig. 5. Results of behavioral identification of termites. Three behaviors were identified: Non-moving (black), random wandering (blue) and forward moving (red).

random wandering, and forward moving (Fig. 5). The behavioral state functions $b_i(t)$ were constructed using these identified behavioral states, as shown in Fig. 6.

To construct the state transition rules, we used the numbers of other nearby individuals in each of the three behavioral states as the environment vector $\vec{e}_i(t)$. The spatial radius of neighbor detection was set to approximate the termite individuals' typical body size, assuming that their individual-to-individual interactions were largely contact-based. We also included a constant unity as the first element of $\vec{e}_i(t)$ so as to be able to detect inherent state transition probabilities that were independent of the influences of nearby individuals. The state transition tensor \hat{T} was estimated using the standard least squares method for each $T_{b_i(t)}$.

The results are shown in Fig. 7, where the strengths of interactions among individuals in local vicinity were success-

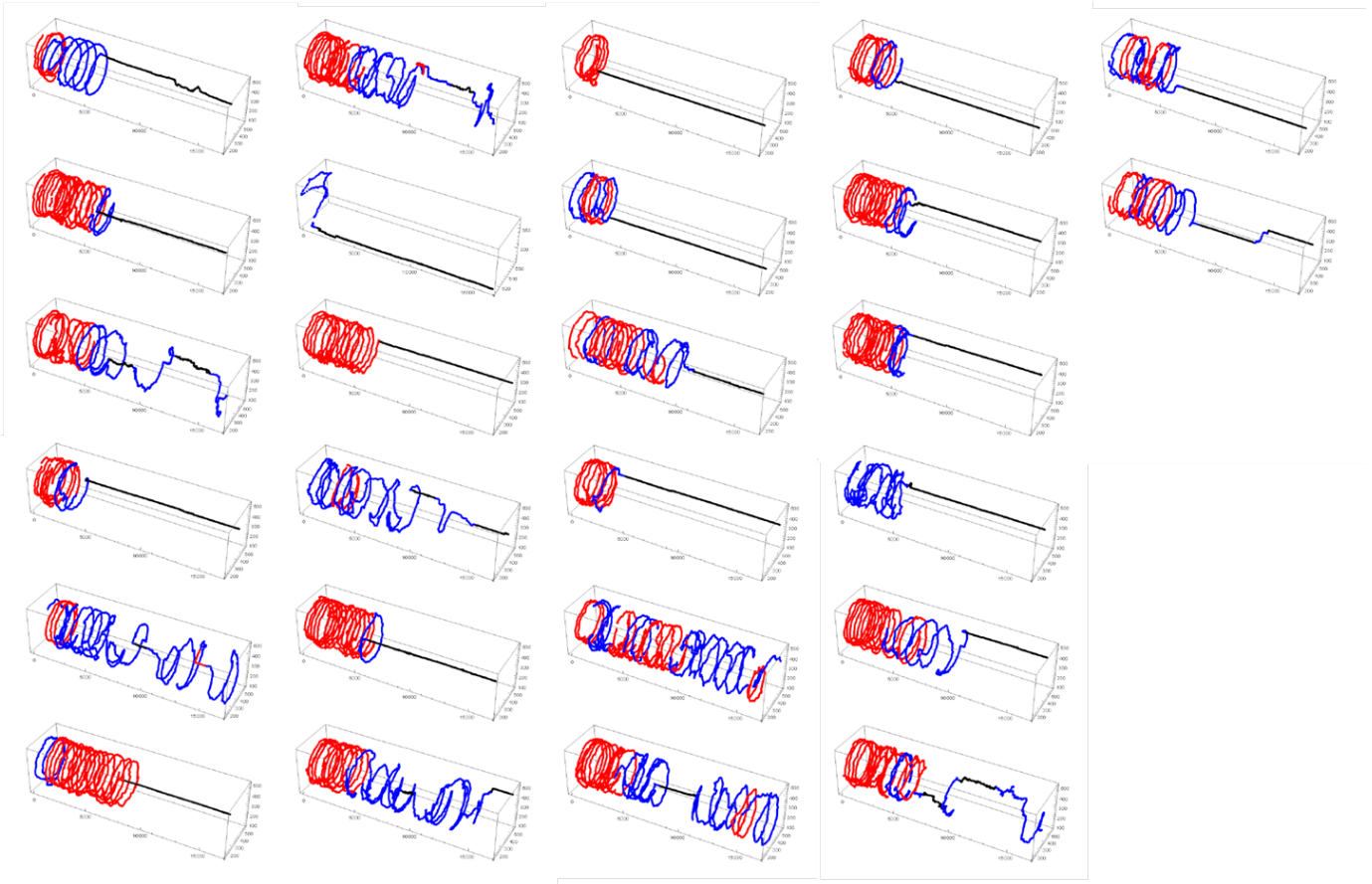


Fig. 6. Behavioral state functions ($b_i(t)$) of 26 termites individuals visualized on each individual trajectory. Time flows from left to right. Behavioral states are indicated by color (non-moving = black, random wandering = blue, and forward moving = red).

		Current state		
		Non-moving	Random wandering	Forward moving
Next state	Non-moving	$\begin{pmatrix} 0.998633 \\ -0.00171597 \\ -0.000068283 \\ 0.00227864 \end{pmatrix}$	$\begin{pmatrix} 0.00673272 \\ 0.00536347 \\ 0.000270352 \\ -0.00245897 \end{pmatrix}$	$\begin{pmatrix} 0.00147674 \\ 0.023784 \\ 0.00120177 \\ -0.000409453 \end{pmatrix}$
	Random wandering	$\begin{pmatrix} 0.00153507 \\ 0.000861908 \\ 0.000470325 \\ -0.00203876 \end{pmatrix}$	$\begin{pmatrix} 0.977766 \\ -0.00220219 \\ -0.00651538 \\ -0.00596974 \end{pmatrix}$	$\begin{pmatrix} 0.0300453 \\ 0.0428533 \\ -0.0051096 \\ -0.0104541 \end{pmatrix}$
	Forward moving	$\begin{pmatrix} -0.000167797 \\ 0.000854058 \\ -0.000402042 \\ -0.000239876 \end{pmatrix}$	$\begin{pmatrix} 0.0155016 \\ -0.00316127 \\ 0.00624503 \\ 0.00842872 \end{pmatrix}$	$\begin{pmatrix} 0.968478 \\ -0.0666372 \\ 0.00390783 \\ 0.0108635 \end{pmatrix}$

Fig. 7. State transition tensor \hat{T} obtained from the trajectories of termites. The tensor was transposed to improve readability. The size of \hat{T} is $3 \times 3 \times 4$. The numbers outside the yellow boxes represent inherent state transition probabilities from one behavioral state (shown at the top) to another (shown on the left). The numbers inside each yellow box represent changes of the state transition probabilities caused by the presence of another individual nearby with each of the three behavioral states (top: non-moving, middle: random wandering, bottom: forward moving, in each box).

fully captured (marked with yellow boxes in Fig. 7). Positive (negative) numbers indicate that the presence of individuals with a particular state will increase (decrease) the state transition probability. For example, the particularly large values circled in blue in Fig. 7 show that, if a forward-moving termite individual faces another individual that is not moving (we can tell this because these numbers appeared in the top row of each yellow box), then the probabilities for state transition to the non-moving or random wandering state will increase significantly. Another example is 0.0108635 at the very bottom to the right in the tensor; this means that, if a forward-moving individual has another running mate nearby that is also forward moving, then the probability of keeping the same state will receive a boost by about 1% (otherwise it would be 96.85%, which is given right above the bottom-right yellow box).

This result illustrates that the proposed method can provide quantitative information about how individuals with various behavioral states interact with each other, and how strong such interactions are, in the biological collective being observed.

IV. APPLICATION II: DETECTING INTERACTIONS AMONG PEDESTRIANS

The second application is to track and model movements of human pedestrians in a university campus. This is to test the applicability of the proposed method to more complex, noisy collectives “in the wild”, with dynamically changing size. As the input data, we recorded pedestrians walking in the central part of the Binghamton University campus during a lunch break for one hour (Fig. 8). The recording was conducted with the Binghamton University IRB approval. During the recorded period of time, a large number of pedestrians entered and moved out of the recorded spatial area, making the size of S , the set of moving individuals, dynamically changing. To make things more complicated, there were several obstacles (e.g., trees, lampposts; see Fig. 8) that would temporarily hide moving individuals, making the tracking task very challenging.

The positions of moving individual pedestrians were tracked using a custom-made image processing program that was developed using OpenCV [10]. First, the background subtraction function of OpenCV was utilized to detect objects that did not belong to the static background. The perspective of the image was then transformed from the birds-eye view to the top view, in which the positions and velocities of the objects were calculated and tracked (Fig. 9).

To enhance the robustness of tracking, we developed an original, hybrid algorithm that combined image processing (for object detection and perspective transformation; implemented with OpenCV) with real-time online agent-based simulation (for motion *prediction* in a noisy dynamic environment; implemented in Python). Specifically, each detected object was internally represented as an agent with its unique position and velocity as agent attributes, and their movements were simulated internally alongside the image processing. After the object detection was completed for each video frame, the locations of the detected objects were compared to those of the simulated agents, and the objects that were close enough to the



Fig. 8. A sample snapshot of birds-eye-view video recordings of pedestrians walking in the Binghamton University campus, taken from the ninth floor of the University’s Library Tower.

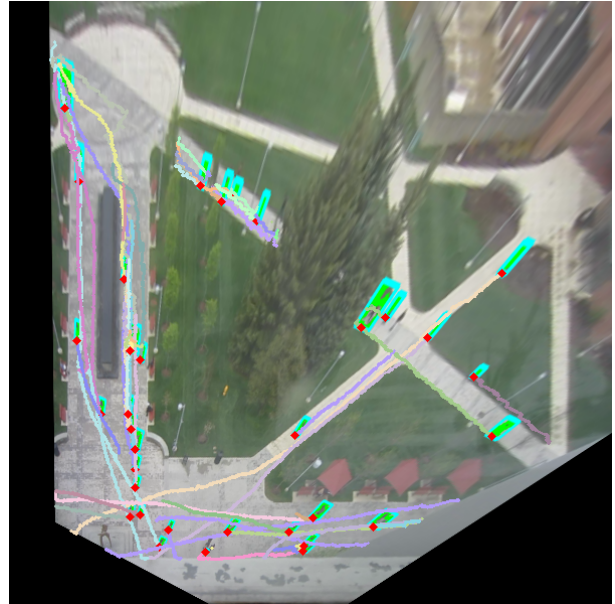


Fig. 9. Transformed top-view video, being analyzed by the hybrid tracking system that combines image processing and online agent-based simulation. Detected pedestrians are highlighted by cyan rectangles, with red dots at the bottom indicating the locations of simulated “agents”. Their trajectories are shown in different colors. Black areas are the outside of the original video frame.

existing agents were “claimed” by those agents, followed by adjustment of the agents’ positions and velocities according to the positions of the claimed objects. Unclaimed objects were represented as new agents (which might be aggregated into other existing agents if their trajectories converged later). The agents that could not claim any object would remain moving along a linear projection, either until it re-claimed an object (in this case the tracking would continue) or until it moved for a certain period of time without claiming an object or moved

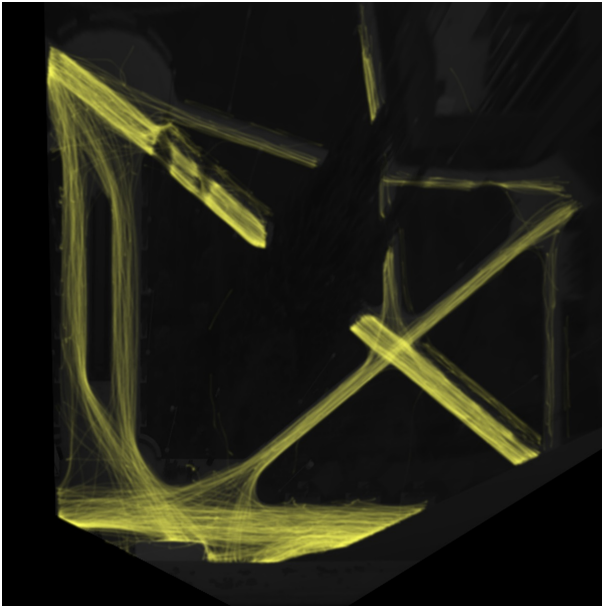


Fig. 10. Reconstructed pedestrian trajectories from one hour of the video recording.

out of the recorded spatial area (in these cases the tracking of the agent would be terminated and its trajectory would be written out into a file). Each of the recorded trajectories was smoothed out using a Gaussian kernel (with standard deviation set to 20 frames $\approx 2/3$ sec.) applied over time to reduce noise. Figure 10 shows an example of the reconstructed pedestrian trajectories.

Figure 11 presents the histogram of the pedestrians' speeds, which shows that most of the pedestrians moved with the speed between 0.1 and 0.5 pixels per frame. We therefore designated the speeds that fell within this range as "normal moving", while the speeds less than 0.1 as "not moving", and those above 0.5 as "fast moving". The two moving categories (normal moving and fast moving) were further classified into eight different directions, given the eight distinct peaks of velocities observed in the velocity distribution (Fig. 12), which reflected the road patterns seen in Fig. 9. As a result, a total of $1 + 8 + 8 = 17$ distinct behavioral states were identified. The trajectories of pedestrians were labeled with these behavioral states based on the speed and direction of their movements.

The trajectories labeled with behavioral states were then analyzed by the same behavioral modeling method as used in the first application, by counting the numbers of other nearby individuals in each of the 17 states and using the least squares method to estimate the state transition matrix for each state. Individuals were considered neighbors if they existed within spatial distance of 30 pixels (≈ 3 m) and temporal distance of 15 frames (≈ 0.5 sec.) from each other. The resulting behavioral transition model was given as a $17 \times 17 \times 18$ tensor (Figs. 13, 14). The majority of transitions were detected in the main diagonal and subdiagonal parts of the tensor (Fig. 14). The main diagonal part corresponds to the maintenance or

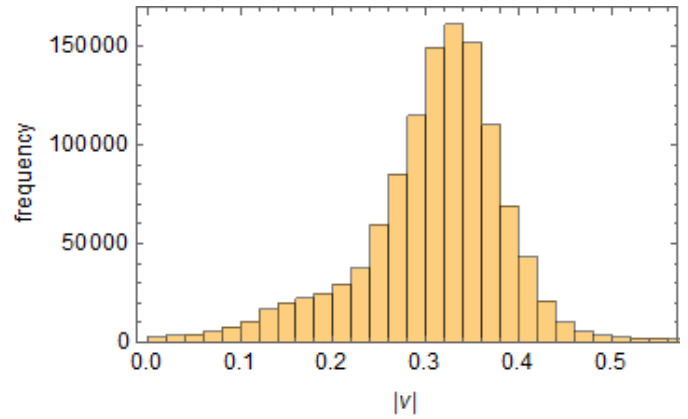


Fig. 11. Histogram of pedestrians' speeds. In most cases, their speeds fell within the range $[0.1, 0.5]$ (unit: pixel per frame).

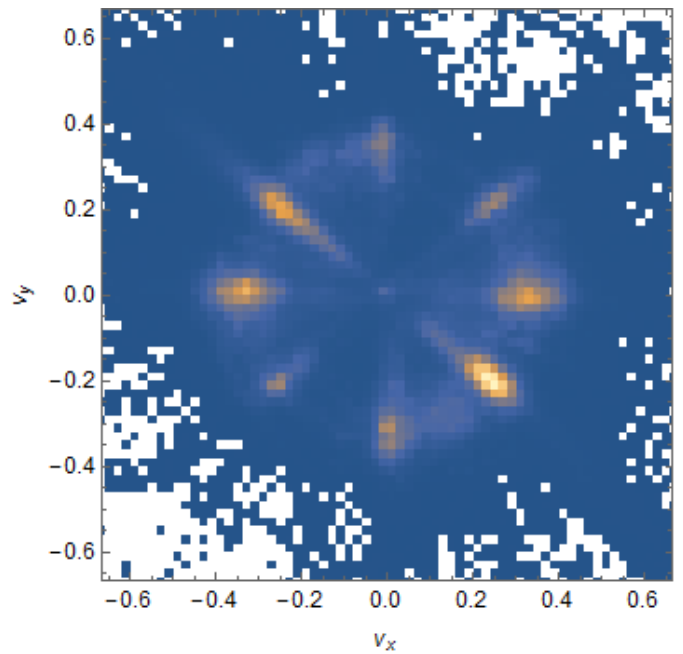


Fig. 12. Density plot showing the distributions of pedestrians' two-dimensional velocities. There were eight clearly established directions, reflecting the road patterns seen in Fig. 9.

minor change of the direction of movement, while the subdiagonal part corresponds to the change of speed between normal and fast moving. A few notable interactions between individuals with different states were also detected, such as having neighbors moving in other directions slows down fast-moving individuals, etc. Overall, the state interactions were generally much less among pedestrians than among termites reported in the previous section. This is because human pedestrians would typically move straight toward an intended destination. This result demonstrated that the developed modeling method and tracking system were able to process collective behaviors in a noisy real-world environment.

V. CONCLUSIONS

In this paper, we have proposed computational approaches to track the movements of biological collectives from ordinary video recordings and to detect and model interactions among individuals with different behavioral states. Our modeling method was based on the assumption that the individuals are finite state machines, which facilitated the identification of behavioral states and the modeling of their state transitions. We conducted a preliminary evaluation of the proposed method through two applications, one for termites and the other for human pedestrians, which both demonstrated the effectiveness of the proposed method and the developed tracking systems.

Needless to say, there are limitations in the present study. Several parameters were involved in the proposed method, such as the spatial/temporal radii used for neighbor detection and the size of the time window for behavioral state characterization, whose effects on the results were not fully explored yet. Also, both the termite and pedestrian examples were observed in highly constrained settings (i.e., termites were confined in a round Petri dish, and pedestrians were moving mostly on simple straight walkways). More systematic evaluations of the effects of parameters and testing the proposed method with video recordings of collective behaviors in less constrained open space will be among our future work. We also plan to conduct critical comparison of our method with other existing tracking/modeling methods.

We believe that the proposed method has potential for practical applications. One application area would be to objectively quantify and compare the strength of local interactions among individuals within biological collectives across multiple species. Another application area would be to detect behavioral anomalies, especially anomalies in interaction patterns, in a crowd of people. Both inter-species comparison of collective behaviors and anomaly detection in interaction patterns of organisms are relatively under-explored research areas. We hope that the proposed method uniquely sheds light on those aspects of collective dynamics to further our understanding of complex systems.

ACKNOWLEDGMENTS

H.S. thanks financial support from the US National Science Foundation (1319152). J.S.T. thanks financial support from the Human Frontiers Science Program (HFSP) (RGP0066/2012).

REFERENCES

- [1] M. Kabra, A. A. Robie, M. Rivera-Alba, S. Branson, and K. Branson, "JAABA: Interactive machine learning for automatic annotation of animal behavior," *Nature Methods*, vol. 10, no. 1, pp. 64–67, 2013.
- [2] A. Pérez-Escudero, J. Vicente-Page, R. C. Hinz, S. Arganda, and G. G. de Polavieja, "idtracker: tracking individuals in a group by automatic identification of unmarked animals," *Nature methods*, vol. 11, no. 7, pp. 743–748, 2014.
- [3] A. I. Dell, J. A. Bender, K. Branson, I. D. Couzin, G. G. de Polavieja, L. P. Noldus, A. Pérez-Escudero, P. Perona, A. D. Straw, M. Wikelski *et al.*, "Automated image-based tracking and its application in ecology," *Trends in Ecology & Evolution*, vol. 29, no. 7, pp. 417–428, 2014.
- [4] M. Vela-Pérez, M. Fontelos, and S. Garnier, "From individual to collective dynamics in Argentine ants (*linepithema humile*)," *Mathematical Biosciences*, vol. 262, pp. 56–64, 2015.



Fig. 13. State transition tensor \hat{T} obtained from the trajectories of pedestrians. The tensor was transposed to improve readability. The size of \hat{T} is $17 \times 17 \times 18$. The format of presentation is the same as in Fig. 7. See Fig. 14 for an enlarged version.

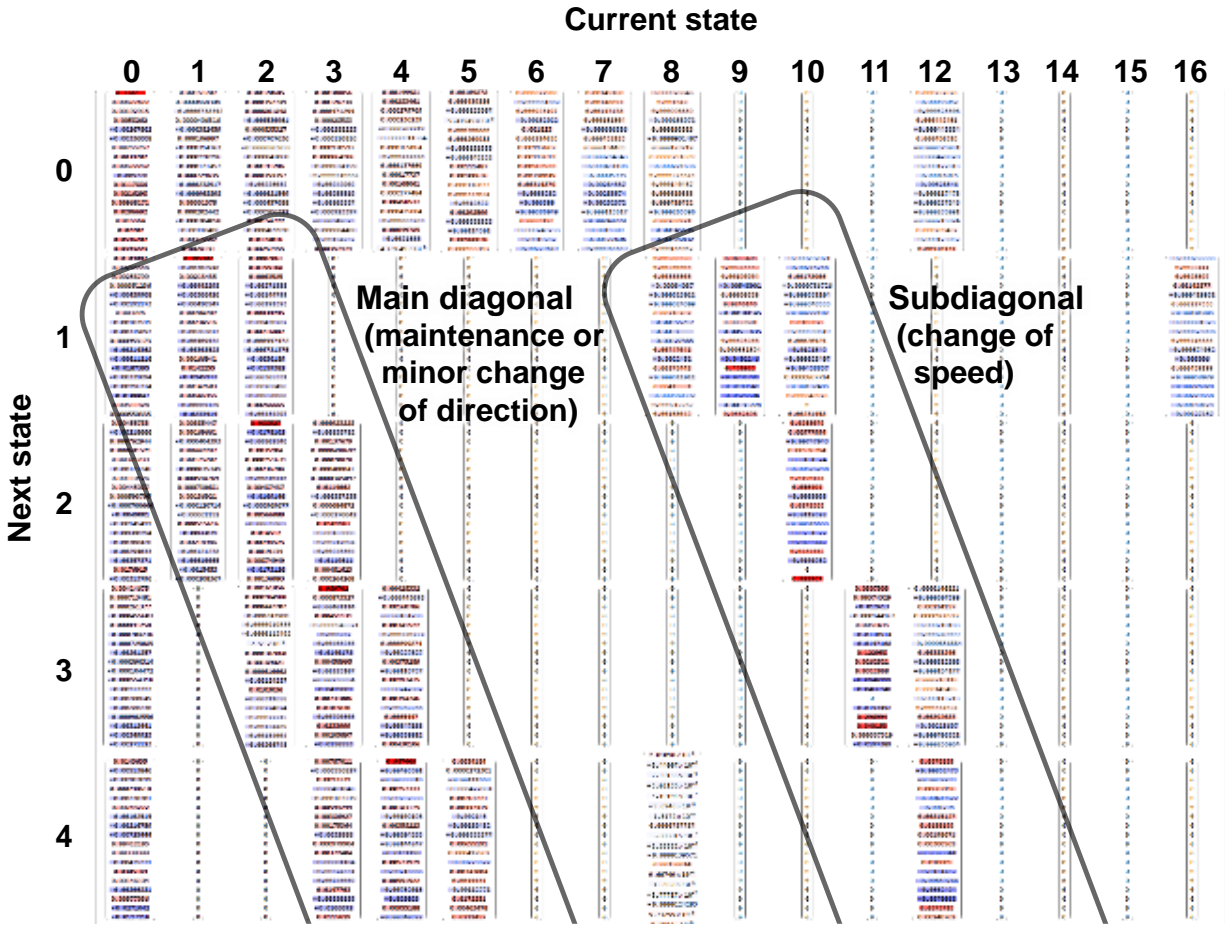


Fig. 14. Enlarged top part of state transition tensor \hat{T} shown in Fig. 13. Red and blue highlights indicate positive and negative coefficients, respectively. Non-zero entries typically appear in the main diagonal and subdiagonal parts; the former corresponds to the maintenance or minor change of the direction of movement, while the latter corresponds to the change of speed between normal and fast moving.

- [5] H. Kunz and C. K. Hemelrijk, "Artificial fish schools: Collective effects of school size, body size, and body form," *Artificial Life*, vol. 9, no. 3, pp. 237–253, 2003.
- [6] H. Sayama, "Swarm chemistry," *Artificial life*, vol. 15, no. 1, pp. 105–114, 2009.
- [7] H. Hamann, T. Schmicke, and K. Crailsheim, "Analysis of swarm behaviors based on an inversion of the fluctuation theorem," *Artificial Life*, vol. 20, no. 1, pp. 77–93, 2014.
- [8] H. Sayama, "Four classes of morphogenetic collective systems," in *ALIFE 14: The Fourteenth Conference on the Synthesis and Simulation of Living Systems*, vol. 14, 2014, pp. 320–327.
- [9] —, "Modeling individual behavioral state transitions from experimental observations of termite collectives," <https://vimeo.com/145404332>, 2015, CoCo seminar talk given on November 11, 2015; accessed on February 29, 2016.
- [10] G. Bradski and A. Kaehler, *Learning OpenCV: Computer Vision with the OpenCV Library*. O'Reilly Media, Inc., 2008.